Combining Electrical and Pressure Measurements for Early Flooding Detection in a PEM Fuel Cell

Giovanni Dotelli, Roberto Ferrero, *Member, IEEE*, Paola Gallo Stampino, Saverio Latorrata, and Sergio Toscani, *Member, IEEE*

***Abstract*— Water flooding is one of the main causes of performance degradation for polymer electrolyte membrane fuel cells (FCs), and its prompt detection is therefore important to guarantee optimal FC operation. This paper aims at comparing the most common methods for flooding diagnosis, which are based on electrical or gas pressure measurements. Their differences in terms of sensitivity to flooding are investigated, primarily focusing on their suitability for its early detection. In particular, the differences between anodic and cathodic pressure drop measurements are highlighted, as well as their relationship with the FC electrical output. The experimental results show that cathodic pressure measurements are the most convenient choice for early flooding detection. Measurements have been performed on a single cell, since it allows an easier interpretation of the results, although the applicability of the considered methods to FC stacks for commercial applications is also discussed.**

***Index Terms*— Diagnostics, fuel cell (FC), impedance spectroscopy, pressure measurements, water management.**

I. Introduction

WATER management is one of the main issues that affect the efficiency and lifetime of polymer electrolyte membrane fuel cells (PEM FCs). In particular, flooding of catalyst or flooding of gas diffusion layers as well as that of gas channels (especially at the cathode) due to an excessive amount of water is one of the most important causes of FC performance degradation during high-current operation [1], [2]. The development of suitable methods to detect flooding early and undertake corrective actions is therefore essential to guarantee proper FC operation, with high efficiency and stable output power, necessary for a massive-scale market diffusion of FC-powered devices.

The most common diagnostic approach in laboratory experiments is based on electrochemical impedance spectroscopy (EIS), which provides a large amount of information about the electrochemical processes characterizing the FC behavior. Indeed, impedance measurements at different frequencies allow distinguishing between the different contributions of voltage drop, and flooding is expected to produce an increase in the low-frequency impedance (typically below 10 Hz), associated with mass transport limitation. For this reason, several papers in the last decade suggested monitoring the low-frequency impedance as an effective technique to detect flooding (see [3]–[6]).

It is, however, known that this method has important limitations. First, low-frequency measurements require a long observation time in steady-state conditions, while flooding conditions are usually characterized by unstable operation with fast and large voltage variations [2], which dramatically affect the measurement accuracy. Second, spectroscopy measurements on the whole cell do not allow distinguishing between the anode and cathode contributions, so it is not possible to identify the main location of flooding, which would be useful to undertake proper corrective actions. Finally, it is worth mentioning that EIS usually requires *ad hoc* instrumentation to generate the ac perturbation, which usually cannot be afforded in commercial applications, although recent research suggested the use of power converters to produce such perturbations with significantly lower costs [7]–[9].

For the above-mentioned reasons, other techniques for flooding diagnosis have been investigated in the recent years and research in this direction is still in progress. An up-to-date review of the proposed diagnostic approaches, also discussing implementation issues, can be found in [10]. Several nonelectrical methods have been developed [11], among which the simplest one from the implementation point of view is based on gas pressure drop measurements between the inlet and outlet channels, usually at the cathode [12]–[14], but also at the anode [15]. First results concerning the development of statistical methods have also been recently published, either based on cell voltage measurements alone [16], [17] or on the correlation between voltage and pressure measurements [18].

Despite the wide literature on the subject, flooding phenomena have not been completely understood yet, and consequently their effects on the physical quantities measured by different diagnostic methods also need further investigation. While several methods have been individually tested and proven to be effective in particular conditions, there is a significant lack of experimental comparative studies in the literature. In particular, there is no general agreement on which pressure measurement (anodic or cathodic) provides better

Manuscript received June 20, 2015; revised September 26, 2015; accepted October 1, 2015. Date of publication November 12, 2015; date of current version April 5, 2016. The Associate Editor coordinating the review process was Dr. Dario Petri.

G. Dotelli, P. Gallo Stampino, and S. Latorrata are with the Department of Chemistry, Materials, and Chemical Engineering G. Natta, Politecnico di Milano, Milan 20133, Italy (e-mail: giovanni.dotelli@polimi.it; paola.gallo@polimi.it; saverio.latorrata@polimi.it).

R. Ferrero is with the Department of Electrical Engineering and Electronics, University of Liverpool, Liverpool L69 3GJ, U.K. (e-mail: roberto.ferrero@liverpool.ac.uk).

S. Toscani is with the Dipartimento di Elettronica, Informazione e Bioingegneria, Politecnico di Milano, Milan 20133, Italy (e-mail: sergio.toscani@polimi.it).

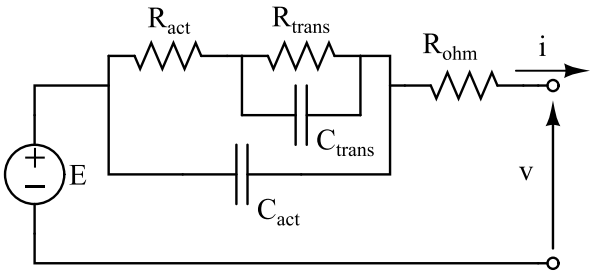

Fig. 1. Linearized equivalent circuit describing the main causes of PEM FC voltage drop, namely, ohmic losses, activation polarization, and mass transport limitations.

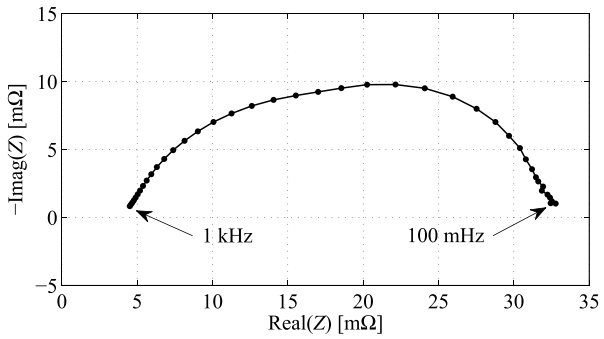

Fig. 2. Typical impedance spectrum of the FC used for the experimental analysis (see Section III), measured at 16.1 A (0.7 A/cm^2) in nonflooded conditions.

results in terms of sensitivity to incipient flooding and to other phenomena that can be monitored to early detect its possible occurrence.

Ferrero *et al.* [19] reported preliminary results aimed at comparing electrical and cathodic pressure measurements, which are the most common approaches and also good candidates for commercial applications because of their low cost and complexity. In more detail, the pressure drop at the cathode was shown to be suitable for an early detection of relative humidity increase in the gases, which can eventually lead to cell flooding. Here, these results are recalled and further discussed, focusing on the features of the measurement signals that can be more reliably considered as good indicators of possible flooding. With regard to this issue, the differences between anodic and cathodic pressure measurements are also investigated. Indeed, the different dynamics at the anode and the cathode give rise to different responses of the two pressure measurements in the presence of liquid water in the cell, and such differences affect the reliability of flooding prediction.

The experimental analysis is carried out on a single PEM FC for an easier interpretation of the measurement results, but the applicability of the considered methods to FC stacks for commercial applications is also briefly discussed.

II. FC Impedance and Gas Pressure Drop

A. Low-Frequency Impedance

The voltage–current relationship of a PEM FC arises from a complex interplay of several physical processes that determine the different causes of voltage drop. The simplest linearized model that includes the three main contributions to the total voltage drop, namely, ohmic losses, activation polarization, and mass transport limitations, is shown in Fig. 1 in terms of electrical equivalent circuit.

The cutoff frequencies of the activation and transport RC circuits are usually well separated so that the three contributions to voltage drop can be individually recognized in the impedance spectrum at different frequencies. In more detail, transport limitations are seen at low frequencies (typically below 10 Hz), while activation polarization is dominant at intermediate frequencies (between 10 Hz and 1 kHz), and finally, the ohmic resistance is the high-frequency limit of the impedance spectrum (neglecting inductive phenomena).

The Nyquist plot of a typical impedance spectrum of the cell used for the experimental analysis described in Section III, in typical operating (nonflooded) conditions, is reported in Fig. 2, in the frequency range from 100 mHz to 1 kHz. The low- and high-frequency arcs are well recognizable, although a better fit of the experimental data with the equivalent circuit model in Fig. 1 would require a constant-phase element instead of the capacitance C_{act} [5] or, equivalently, a frequency-dependent capacitance $C_{\text{act}}(j\omega)$ [20], [21]. However, these details are out of the purposes of this paper, which does not deal with activation processes.

According to the literature, a combined monitoring of the low- and high-frequency impedances, by acquiring either the whole spectrum [3]–[5] or single-frequency impedances [6], is generally believed to be an effective approach to distinguish between drying and flooding, as membrane dehydration causes an increase in the membrane ionic resistance and, therefore, in the cell equivalent ohmic resistance, whereas the worse mass transport due to cell flooding is expected to increase the low-frequency impedance. However, while the relationship between membrane humidity and ohmic resistance is quite straightforward and well understood, the relationship between cell flooding and low-frequency impedance is more complex and requires further discussion. In fact, flooding is promoted by a noneffective water removal by gas flow, and for this reason, gas flow rates lower than usual (especially at the cathode) are often chosen in flooding experiments. In these conditions, fuel (at the anode) or oxygen (at the cathode) starvation, with a consequent significant increase in the low-frequency impedance, is likely to occur even without flooding. Therefore, it is difficult to identify whether any observed impedance increase is actually due to flooding, leading to possible misinterpretation of the measurement results, as shown in Section III-B.

Finally, it is worth mentioning that high- and low-frequency impedance measurements for drying and flooding diagnosis, respectively, are also different from the implementation point of view. While the former can be obtained by exploiting the high-frequency ripple that is produced by switch-mode power converters connected to most FCs in commercial applications [8], [22], [23], the latter requires dedicated instrumentation to produce the low-frequency perturbation or *ad hoc* control of the switch-mode converters in order to superimpose low-frequency components onto the ripple waveform, thus increasing the system complexity, cost, and power losses.

For all these reasons, high-frequency impedance measurements can be effectively employed for membrane drying diagnosis without significant drawbacks concerning data interpretation, system complexity, or FC performance, while for flooding diagnosis, alternative solutions to low-frequency impedance measurements may represent a more convenient choice in some applications.

B. Gas Pressure Drop at the Anode and the Cathode

The pressure drop between inlet and outlet gases arises from the friction that the gas experiences in its path along the FC flow field and gas diffusion layer. Despite the complexity of the underlying phenomena determining the gas path within the cell and the differences arising from different flow field designs, a simple and general explanation of the effects of flooding can be formulated as follows. The accumulation of liquid water in the gas path decreases the equivalent cross section available for the gas flow, and thus it results in a pressure increase in the inlet channel. For this reason, pressure drop measurements have been suggested in the literature as a simple and effective approach to detect cell flooding.

Since the FC chemical reaction produces water at the cathode, flooding is often believed to be more likely to occur there, particularly during the high-current operation. For this reason, most works in the literature chose to measure the cathodic pressure drop for flooding diagnosis [12]–[14]. However, the chemical reaction is not the only source of water, as inlet gases are usually humidified, particularly at the anode; moreover, transport phenomena across the membrane, such as back diffusion, allow water to move from the cathode to the anode, while electro-osmotic drag favors water transport from the anode to the cathode [24]. Therefore, flooding may also occur at the anode [25], and depending on the cell design, anodic pressure measurements may be considered more suitable for its detection [15].

For both anodic and cathodic measurements, however, the relationship between pressure drop and FC electrical output is not straightforward. Thus, further investigations are required in order to achieve a reliable flooding detection based on pressure measurements. Indeed, while a pressure drop increase can be reasonably associated with a gas relative humidity increase, this does not always imply a decrease in the FC output power, as experimentally confirmed in the following section. The reason for this is probably that the presence of liquid water can have very different effects depending on its position within the cell, while the effect on the externally measured pressure is always similar.

In more detail, the pressure drop that is measured across the cell both at the anode and the cathode simply corresponds to an increase in gas pressure in the flow field channels, but this does not necessarily entail limitations of reactants to the catalytic layer. Only flooding of the gas diffusion layer can prevent reactant gases from reaching the reaction site, and this has an impact on FC output power. Therefore, it is important to distinguish between the case where gas pressure increases, but reactants are still largely available in the whole cell surface, and the case when full clogging of the channel occurs inside the cell causing a substantial reduction of the active area [26]. In the former case, the gas pressure increase can even have a positive effect on the FC output power because pressure favors cell potential. In the latter case, the overall effect on FC performances is potentially negative; for instance, the local reaction rate where gas is still fed is bound to accelerate in constant-current mode and the consequences are different depending on the cell side where this clogging occurs. At the cathode side, there would be a local increase in water production and a possible worsening of flooding conditions that only back transport of water toward the anode could counterbalance; however, because the driving force in this case would be water chemical potential across the membrane, the use of highly humidified hydrogen would nullify the effect and cathode flooding would be a more likely consequence that only high flow rates could help avoid. On the contrary, at the anode side, there would be an increased electro-osmotic drag that helps water removal; then, flooding could be prevented in normal conditions even at relatively low flow rates typical of hydrogen feeding. This is not the case if the cell is operated in dead-end mode, as it is often done not to waste precious hydrogen. In this case, regular purge is necessary [15].

Unfortunately, it is very difficult to predict whether and where flooding is likely to occur, simply on the basis of operating conditions because many parameters are influencing water management [15]: current density, cell temperature, gas flow rate, stoichiometry, and humidity content, just to quote the most relevant ones. Thus, effective diagnostic methods to early detect flooding occurrence are particularly desirable.

The experimental analysis reported in the next section also aims at addressing these issues and finding peculiar features of the pressure signals that can be considered more directly related to the FC electrical performance. Thus, a flooding detection based on them would allow a more reliable diagnosis.

III. Experimental Results and Discussion

A. Experimental Setup

For a better interpretation of the measurement results, a single PEM FC (Fuel Cell Technologies) was chosen for the experimental analysis. The applicability of the considered diagnostic approaches to FC stacks for commercial applications is then briefly discussed.

The cell has an active area of 23 cm^2, and it is composed of commercial materials, in particular a Nafion 212 membrane as electrolyte (50-μm thickness) and a gas diffusion electrode reference sample (E-TEK LT140). Pure hydrogen and air are fed into the anode and the cathode, respectively, whose flow rates are measured and controlled by calibrated flow meters. Both inlet gases are humidified through saturators, whose temperatures are controlled to achieve the desired relative humidities. The pressures of the gases are measured at both the anode and the cathode where they enter the cell, by piezoresistive pressure sensors (Bürkert 8323); since the outlet gases are freely discharged into the atmosphere, such measurements provide the pressure drops across the cell. Finally, the cell temperature is also controlled.

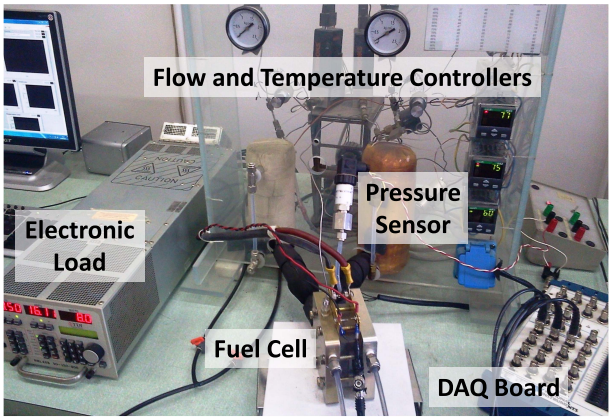

Fig. 3. Photograph of the experimental setup.

The electrical output of the cell is connected to an electronic load (TDI RBL488-50-150-800) that imposes the output current and also provides its measurement as a voltage signal. Such a signal, together with the cell voltage and the pressure measurements provided by the pressure sensors, is acquired by a multifunctional 16-bit data acquisition (DAQ) system (NI 6259), with a sampling frequency of $1 \cdot 10^5$ samples/s. The same DAQ system is also used to generate the reference signal for the electronic load. A picture of the whole experimental setup is shown in Fig. 3.

The FC was operated at a medium–high constant current of 16.1 A (0.7 A/cm^2), in order to have a significant water production at the cathode, and at a constant temperature of 60 °C. The relative humidity of the inlet gases was 80% at both the anode and the cathode, empirically chosen to keep the membrane well humidified without flooding the cell. The typical impedance spectrum shown in Fig. 2 was obtained in these conditions, with high flow rates, namely, 0.2 Nl/min for hydrogen and 1.0 Nl/min for air, corresponding to the stoichiometric ratios (λ) of 1.8 and 3.8, respectively, chosen in order to guarantee a highly stable operation, necessary to obtain accurate impedance measurements at low frequencies. On the contrary, for flooding tests, the gas flow rates were set at 0.13 Nl/min for hydrogen and 0.54 Nl/min for air, corresponding to stoichiometric ratios of 1.2 and 2.0, respectively. These values were high enough to allow a reasonably stable operation, without being so high to prevent flooding by removing a large amount of excess water.

The two extreme frequencies of the spectrum, i.e., 100 mHz and 1 kHz, were chosen to monitor the low-frequency impedance for FC flooding diagnosis and the ohmic resistance for membrane dehydration diagnosis, respectively. Thus, a multisine perturbation was superimposed onto the FC dc current, composed of a 100-mHz harmonic component with a 100-mA amplitude and a 1-kHz harmonic component with a 250-mA amplitude. The greater amplitude at high frequency is allowed by the response linearity at this frequency, and it is justified considering that the magnitude of the voltage response at higher frequency is smaller. As far as the low-frequency impedance is concerned, it is worth mentioning that some papers in the literature prefer to use the imaginary part of the impedance at a higher frequency (where the imaginary part is higher) as an indicator of flooding [6], because it is in principle not affected by possible ohmic resistance variations. However, if the ohmic resistance is simultaneously measured, its effects can be easily compensated for (even in the time domain [27]) and the other contributions to the low-frequency impedance can be accurately evaluated. Moreover, impedances at lower frequencies are generally more sensitive to flooding.

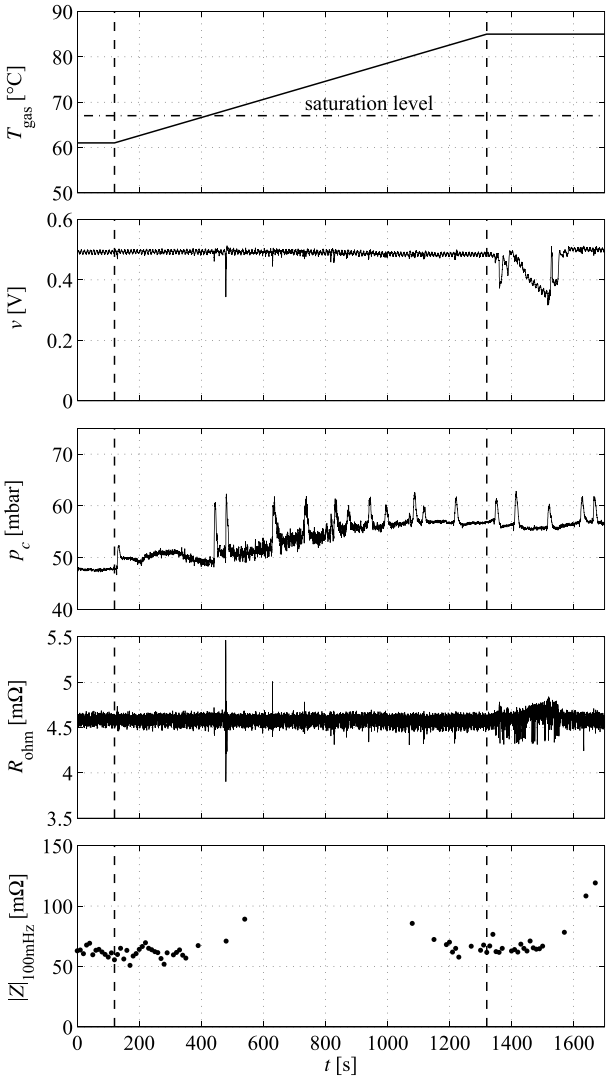

Fig. 4. FC voltage (second plot), cathodic pressure drop (third plot), ohmic resistance (fourth plot), and absolute value of the 100-mHz impedance (fifth plot) measured during a flooding transient induced by the gas temperature increase shown in the first plot. Only the significant values of the 100-mHz impedance are plotted.

B. Cathodic Pressure Versus Low-Frequency Impedance

The first flooding test aiming at comparing the two most common measurements performed in the literature, namely, cathodic pressure and low-frequency impedance, is reported in Fig. 4. The flooding transient was induced by gradually increasing the inlet gas relative humidity from 80% to supersaturated conditions, at both the anode and the cathode, by increasing the gas temperature in the saturators as shown in the first plot of Fig. 4.

The cell voltage, the cathodic pressure drop, the real part of the 1-kHz impedance (ohmic resistance estimate), and the absolute value of the 100-mHz impedance are also reported in Fig. 4. All quantities were averaged on a time window of 0.1 s, except for the 100-mHz impedance, whose values were calculated every 10 s (waveform period). It is apparent that the voltage instabilities arising in flooding conditions cause significant distortions in the low-frequency voltage response, as already mentioned, and therefore they prevent from always obtaining accurate impedance measurements. Thus, the total harmonic distortion (THD) index was calculated for each 10 s period of the voltage waveform (considering only the first 100 harmonic components for the calculation) and only the impedance values corresponding to a THD lower than 30% are actually plotted in Fig. 4 (the current THD was always well below 1% as the current was imposed by the electronic load). Even at the beginning of the transient, these values are much greater than the 100-mHz impedance in Fig. 2. This increase is due to the lower gas flow rates, and it must not be confused with the effects of flooding that appear later.

Fig. 4 clearly confirms that the pressure drop begins to increase as soon as the relative humidity of the inlet gases is increased, and it seems to reach a new equilibrium value when the gas humidity stabilizes. It is worth noting that such a pressure increase does not correspond, however, to any significant voltage variation (except for the fast transients), which appears much later, when the pressure is almost constant. This indirect relationship between pressure and FC electrical output needs to be carefully taken into account when using pressure measurements for flooding diagnosis, and it will be further discussed in the next sections.

As far as the impedance is concerned, the ohmic resistance remains practically constant during the whole transient, as expected because, when the membrane is well humidified, a further increase in the gas relative humidity does not produce any significant conductivity increase. On the other hand, the low-frequency impedance is expected to increase due to the worse gas transport caused by the presence of liquid water. In order to better analyze the part of the transient in which flooding actually occurs, a zoomed-in view of it is reported in Fig. 5. Because of the nonstationary conditions of the system, a better estimate of the 100-mHz impedance during the transient can be evaluated from a time-domain fitting of the voltage waveform with a ramp superimposed onto the sine wave. The results thus obtained during flooding (between $t = 1420$ and 1510 s) are reported in Fig. 5, compared with the impedance values before the voltage decrease (between $t = 1240$ and 1340 s).

This comparison confirms that there is an increase in the low-frequency impedance, which, however, is small compared with the high measurement uncertainty arising from unstable operating conditions. Moreover, such an impedance increase is only noticeable when a significant voltage drop due to flooding has already occurred, and it is not suitable for early flooding detection, because in the first stage of the transient, the measurement uncertainty is even higher and the impedance increase (if present) is much smaller.

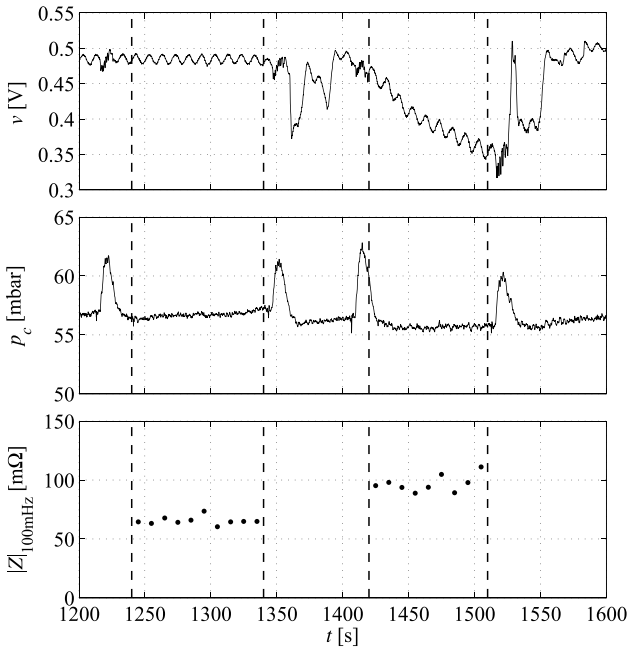

Fig. 5. Enlarged view of part of the transient shown in Fig. 4. The 100-mHz impedance between $t = 1420$ and 1510 s was evaluated by compensating for a ramp voltage decrease.

It could be argued that a choice of a slightly higher frequency for impedance measurement could allow decreasing the uncertainty because of the shorter measurement time, but the sensitivity to flooding would be smaller too. Therefore, it is possible to conclude that the ratio between sensitivity and uncertainty of low-frequency impedance measurements is generally small except when significant flooding has already occurred, and it prevents from employing such measurements for early flooding detection.

C. Variability of Flooding Transients

According to Fig. 4, a cathodic pressure drop increase appears to be a suitable indicator of a possible incipient flooding. However, such information does not allow a reliable flooding prediction, because the complexity of the phenomena leading to flooding, summarized in Section II-B, gives rise to a huge variability of the flooding transients. As examples of such variability, different results obtained in response to the same gas humidity transient are reported in this section, also including the anodic pressure measurement for a more complete analysis.

First, it should be noted that very often (at least 50% of the times, according to the authors' experience), a gas humidity increase is not followed by any significant voltage drop (except for the fast transients), although pressure transients similar to that reported in Fig. 4 are observed, particularly at the cathode. Even when an actual flooding occurs, with a significant voltage drop, the relationship between voltage and pressure measurements may be different from case to case.

As an example, Fig. 6 shows one of such transients, in which a much greater voltage drop occurs (down to 0 V), compared with the transient in Fig. 4, but after a much longer time after the end of the gas humidity transient. Interestingly, the

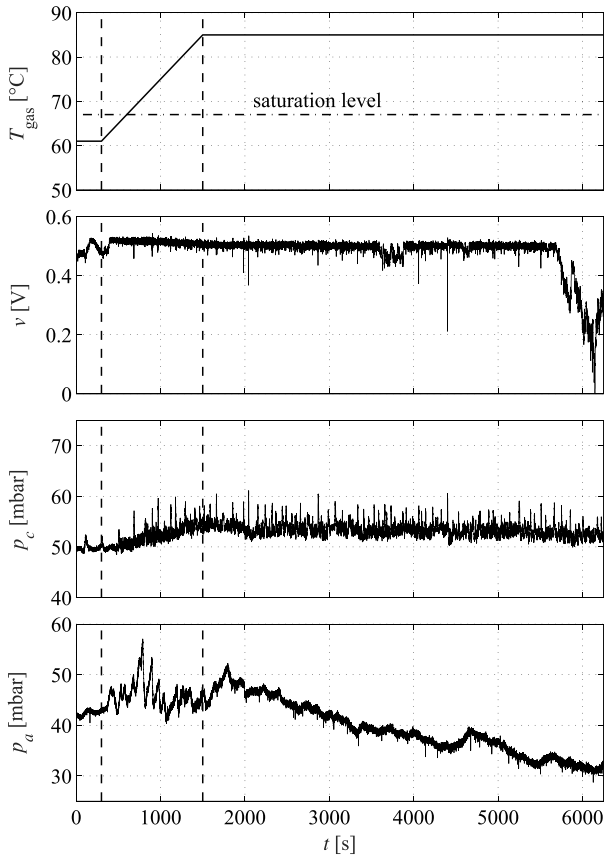

Fig. 6. FC voltage (second plot), cathodic pressure drop (third plot), and anodic pressure drop (fourth plot) measured during the second flooding transient induced by the gas temperature increase shown in the first plot.

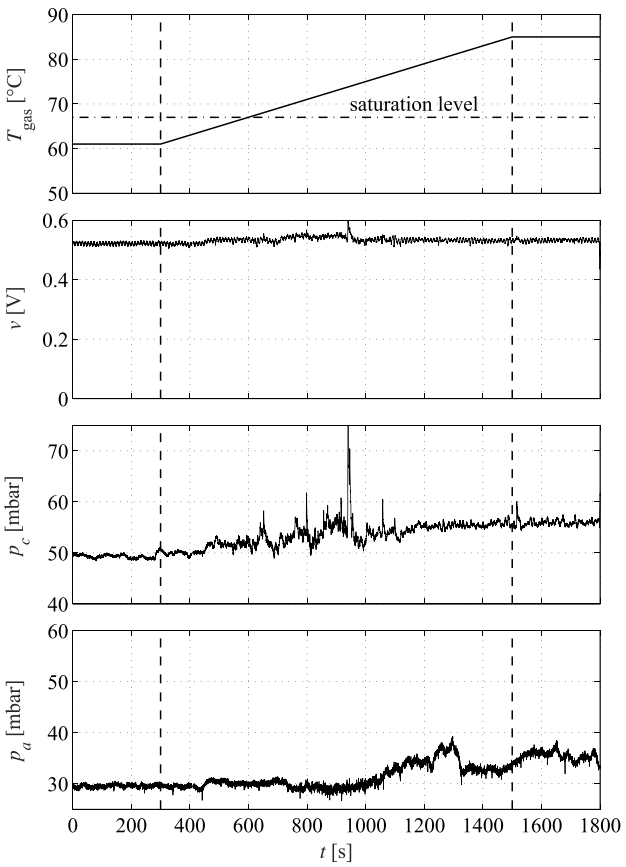

Fig. 7. FC voltage (second plot), cathodic pressure drop (third plot), and anodic pressure drop (fourth plot) measured during the first stage of a flooding transient induced by the gas temperature increase shown in the first plot.

cathodic pressure drop increase is smaller compared with Fig. 4, showing that there is no proportionality between voltage decrease and pressure increase. Moreover, the anodic pressure drop decreases instead of increasing as it would be expected. With regard to this point, it is important to note that at the anode, the flow rate is much smaller than at the cathode, and this allows wider and unpredictable oscillations of the anodic pressure drop. Moreover, at the high current used for these tests, the electro-osmotic drag is an effective water transport mechanism from the anode to the cathode, dominating over back diffusion from the cathode to the anode. This could lead to anode dehydration even if the inlet hydrogen relative humidity is increased, and this makes flooding at the anode an unlikely event [25]. This consideration combined with the natural pressure drop oscillations may explain the observed anodic pressure decrease.

Another example is reported in Fig. 7, in which both cathodic and anodic pressures slightly increase, but there is no significant voltage drop (on the contrary, a small voltage increase can be observed) and even no fast voltage transients as those visible in Figs. 4 and 6. While further confirming the relationship between voltage and pressure that is not straightforward, this result may suggest that the absence of fast voltage dips could indicate that liquid water has not penetrated into the gas diffusion layer, and therefore it does not affect the FC electrical output, as explained in Section II-B.

D. Fast Pressure Transients for Early Flooding Detection

While the slow pressure variations are not always correlated with significant voltage transients, according to what discussed above, the fast spikes in the pressure signals visible in Figs. 4 and 6 correspond to simultaneous voltage dips. Assuming that fast pressure and voltage variations can be considered as the consequence of liquid water reaching the gas diffusion layer, they are good candidates to be reliable indicators of incipient flooding. In this case, combining voltage and pressure measurements could provide further information about the location (anode or cathode) of liquid water, thus allowing undertaking proper corrective actions, such as decreasing the relative humidity of hydrogen or air.

As an example of such differences between the anode and the cathode, Fig. 8 shows some rapid pressure and voltage changes appearing in the second stage of a flooding transient, after the main gas pressure transient has ended. It can be clearly observed that some voltage dips correspond to simultaneous spikes in the cathodic pressure, whereas others correspond to spikes in the anodic pressure. This can be explained by assuming that the pressure spikes arise from a temporary water clog occurring at the anode or the cathode, depending on which pressure signal contains the spike.

The anodic and cathodic spikes have also different dynamics, as shown in Fig. 9, which reports an enlarged zoomed-in view of two spikes appearing in Fig. 8. In more

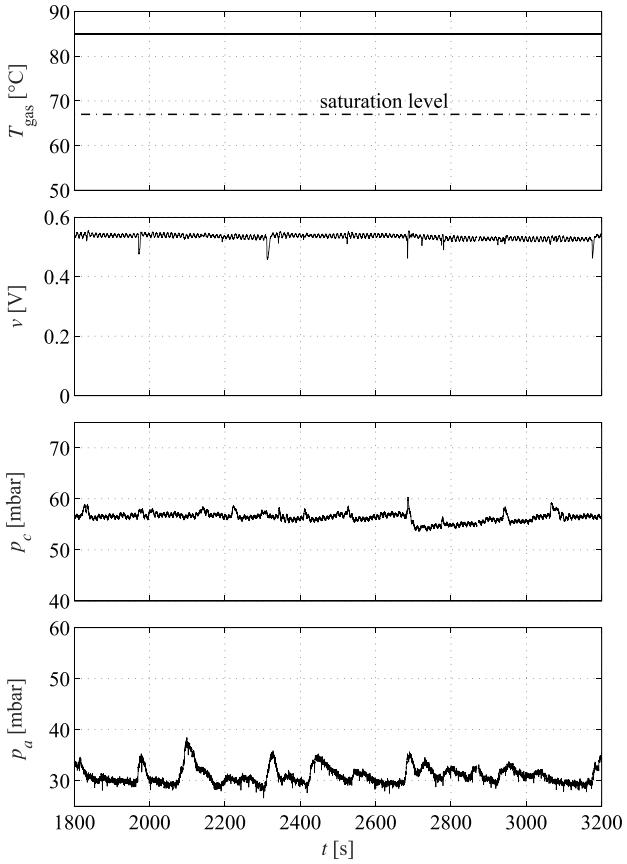

Fig. 8. FC voltage (second plot), cathodic pressure drop (third plot), and anodic pressure drop (fourth plot) measured during the second stage of a flooding transient, when the gas temperature transient has already ended (first plot).

detail, the cathodic pressure variations are much steeper than the anodic ones (there is approximately one order of magnitude difference in both voltage and pressure signals). This is in good agreement with the explanation formulated above. Indeed, the higher gas flow rate at the cathode produces a faster pressure increase in response to the appearance of a water clog, and for the same reason, the clog is eliminated in a shorter time.

Combined voltage and pressure measurements can therefore early detect the location of a possible incipient flooding. It could be argued that the voltage signal alone could provide the same information even without pressure measurements because of the different spike dynamics discussed above. However, thinking about an automatic diagnostic system for commercial applications, the detection of a spike occurrence is a much simpler task than making a decision according to its shape and duration. Moreover, pressure spikes are usually more sensitive to flooding than voltage dips, and they all have similar amplitudes, while the corresponding voltage dips may have very different amplitudes, as visible in Fig. 4. Again, this can be explained by differences in the water clog location within the cell. Thus, combined voltage and pressure measurements should be preferred.

It is worth noting that pressure and voltage measurements can also be performed on an FC stack composed of several cells, typically employed in commercial applications. Pressure measurements can be a global indicator of the overall

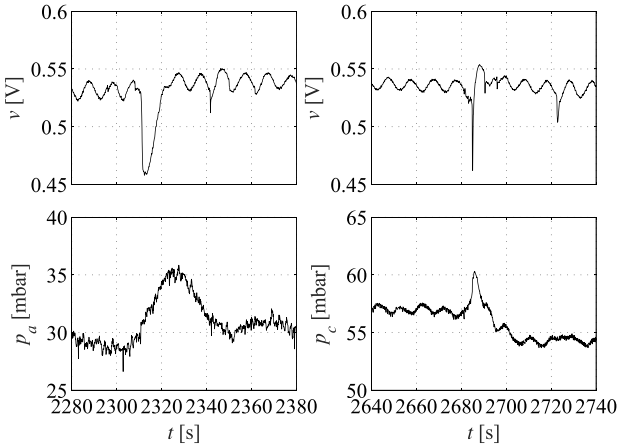

Fig. 9. Enlarged view of voltage (top plots) and pressure (bottom plots) spikes at the anode (left) and the cathode (right) shown in Fig. 8.

water content in the stack, while voltage measurements can be easily performed on single cells or on small groups of cells, depending on the stack size. This is particularly important because water management in stacks is more complex than in single cells since it is rather difficult to obtain an even distribution of the gases and a uniform temperature, meaning that some cells are more prone to flooding than the others. Finally, it should be noted that in the case of FC stacks composed of a large number of cells, pressure measurements may become less sensitive to water clogs (the spikes may have smaller amplitudes), while voltage dips can still be easily detected in measurement signals acquired from single cells or small groups of cells.

If necessary, in order to decrease costs, only one pressure measurement could be performed. In this case, cathodic pressure should be preferred, because the spikes can be easily detected there, thus allowing deducing anodic spikes by exclusion. On the contrary, because of the slower dynamics, anodic spikes can be confused with other pressure variations on similar time scales, not affecting the cell voltage. This can be observed in Fig. 8, where the pressure increase around $t = 2100$ s is similar to that around $t = 2000$ s, but it does not correspond to any voltage dip.

IV. Conclusion

Diagnostic methods for flooding detection in PEM FCs based on electrical and pressure measurements were discussed and experimentally compared on a single cell. A flooding transient was induced by increasing the relative humidities of the inlet gases while continuously monitoring the cell voltage, the ohmic resistance, the 100-mHz impedance, and the cathodic and anodic pressure drops.

Low-frequency impedance measurements, which are often suggested as suitable candidates for flooding diagnosis, were shown to be able to detect flooding only after a significant voltage drop has occurred, and thus they are not suitable for early flooding detection. This is due to the small sensitivity to flooding, compared with the high measurement uncertainty arising from the unstable conditions

that characterize the FC behavior from the first stage of a flooding transient. Also considering the high cost and complexity associated with such measurements, other alternatives should be preferred.

Among these, cathodic pressure measurements were shown to be highly sensitive to gas relative humidity increase at an early stage of the flooding transient. However, such an increase does not always imply an incipient flooding, because it depends on the location of liquid water within the cell. On the other hand, fast pressure spikes (at both the anode and the cathode) corresponding to voltage dips are better indicators of possible incipient flooding, and they can be monitored for a reliable diagnosis. The different dynamics at the anode and the cathode make cathodic spikes more easily recognizable, and therefore cathodic measurements should be preferred if cost and complexity issues prevent from monitoring both anodic and cathodic pressures.

REFERENCES

[1] W. Dai *et al.*, "A review on water balance in the membrane electrode assembly of proton exchange membrane fuel cells," *Int. J. Hydrogen Energy*, vol. 34, no. 23, pp. 9461–9478, 2009.

[2] H. Li *et al.*, "A review of water flooding issues in the proton exchange membrane fuel cell," *J. Power Sour.*, vol. 178, no. 1, pp. 103–117, 2008.

[3] J.-M. Le Canut, R. M. Abouatallah, and D. A. Harrington, "Detection of membrane drying, fuel cell flooding, and anode catalyst poisoning on PEMFC stacks by electrochemical impedance spectroscopy," *J. Electrochem. Soc.*, vol. 153, no. 5, pp. A857–A864, 2006.

[4] W. Mérida, D. A. Harrington, J. M. Le Canut, and G. McLean, "Characterisation of proton exchange membrane fuel cell (PEMFC) failures via electrochemical impedance spectroscopy," *J. Power Sour.*, vol. 161, no. 1, pp. 264–274, 2006.

[5] N. Fouquet, C. Doulet, C. Nouillant, G. Dauphin-Tanguy, and B. Ould-Bouamama, "Model based PEM fuel cell state-of-health monitoring via ac impedance measurements," *J. Power Sour.*, vol. 159, no. 2, pp. 905–913, 2006.

[6] T. Kurz, A. Hakenjos, J. Krämer, M. Zedda, and C. Agert, "An impedance-based predictive control strategy for the state-of-health of PEM fuel cell stacks," *J. Power Sour.*, vol. 180, no. 2, pp. 742–747, 2008.

[7] G. Dotelli, R. Ferrero, P. G. Stampino, S. Latorrata, and S. Toscani, "Diagnosis of PEM fuel cell drying and flooding based on power converter ripple," *IEEE Trans. Instrum. Meas.*, vol. 63, no. 10, pp. 2341–2348, Oct. 2014.

[8] G. Dotelli, R. Ferrero, P. G. Stampino, S. Latorrata, and S. Toscani, "PEM fuel cell drying and flooding diagnosis with signals injected by a power converter," *IEEE Trans. Instrum. Meas.*, vol. 64, no. 8, pp. 2064–2071, Aug. 2015.

[9] N. Katayama and S. Kogoshi, "Real-time electrochemical impedance diagnosis for fuel cells using a DC–DC converter," *IEEE Trans. Energy Convers.*, vol. 30, no. 2, pp. 707–713, Jun. 2015.

[10] C. Cadet, S. Jemeï, F. Druart, and D. Hissel, "Diagnostic tools for PEMFCs: From conception to implementation," *Int. J. Hydrogen Energy*, vol. 39, no. 20, pp. 10613–10626, 2014.

[11] J. St-Pierre, "PEMFC in situ liquid-water-content monitoring status," *J. Electrochem. Soc.*, vol. 154, no. 7, pp. B724–B731, 2007.

[12] W. He, G. Lin, and T. Van Nguyen, "Diagnostic tool to detect electrode flooding in proton-exchange-membrane fuel cells," *AIChE J.*, vol. 49, no. 12, pp. 3221–3228, 2003.

[13] F. Barbir, H. Gorgun, and X. Wang, "Relationship between pressure drop and cell resistance as a diagnostic tool for PEM fuel cells," *J. Power Sour.*, vol. 141, no. 1, pp. 96–101, 2005.

[14] K. Ito, K. Ashikaga, H. Masuda, T. Oshima, Y. Kakimoto, and K. Sasaki, "Estimation of flooding in PEMFC gas diffusion layer by differential pressure measurement," *J. Power Sour.*, vol. 175, no. 2, pp. 732–738, 2008.

[15] M. Song, P. Pei, H. Zha, and H. Xu, "Water management of proton exchange membrane fuel cell based on control of hydrogen pressure drop," *J. Power Sour.*, vol. 267, pp. 655–663, Dec. 2014.

[16] B. Legros, P.-X. Thivel, Y. Bultel, and R. P. Nogueira, "First results on PEMFC diagnosis by electrochemical noise," *Electrochem. Commun.*, vol. 13, no. 12, pp. 1514–1516, 2011.

[17] J. Kim, I. Lee, Y. Tak, and B. H. Cho, "State-of-health diagnosis based on Hamming neural network using output voltage pattern recognition for a PEM fuel cell," *Int. J. Hydrogen Energy*, vol. 37, no. 5, pp. 4280–4289, 2012.

[18] S. Giurgea, R. Tirnovan, D. Hissel, and R. Outbib, "An analysis of fluidic voltage statistical correlation for a diagnosis of PEM fuel cell flooding," *Int. J. Hydrogen Energy*, vol. 38, no. 11, pp. 4689–4696, 2013.

[19] R. Ferrero, S. Toscani, G. Dotelli, P. G. Stampino, and S. Latorrata, "Comparison between electrical and pressure measurements to detect PEM fuel cell flooding," in *Proc. IEEE I2MTC*, Pisa, Italy, May 2015, pp. 1825–1830.

[20] R. Ferrero, M. Marracci, M. Prioli, and B. Tellini, "Simplified model for evaluating ripple effects on commercial PEM fuel cell," *Int. J. Hydrogen Energy*, vol. 37, no. 18, pp. 13462–13469, 2012.

[21] R. Ferrero, M. Marracci, and B. Tellini, "Single PEM fuel cell analysis for the evaluation of current ripple effects," *IEEE Trans. Instrum. Meas.*, vol. 62, no. 5, pp. 1058–1064, May 2013.

[22] G. Dotelli, R. Ferrero, P. G. Stampino, S. Latorrata, and S. Toscani, "Low-cost PEM fuel cell diagnosis based on power converter ripple with hysteresis control," *IEEE Trans. Instrum. Meas.*, vol. 64, no. 11, pp. 2900–2907, Nov. 2015.

[23] M. Hinaje, I. Sadli, J.-P. Martin, P. Thounthong, S. Raël, and B. Davat, "Online humidification diagnosis of a PEMFC using a static DC–DC converter," *Int. J. Hydrogen Energy*, vol. 34, no. 6, pp. 2718–2723, 2009.

[24] G. J. M. Janssen and M. L. J. Overvelde, "Water transport in the proton-exchange-membrane fuel cell: Measurements of the effective drag coefficient," *J. Power Sour.*, vol. 101, no. 1, pp. 117–125, 2006.

[25] S. Ge and C.-Y. Wang, "Liquid water formation and transport in the PEFC anode," *J. Electrochem. Soc.*, vol. 154, no. 10, pp. B998–B1005, 2007.

[26] F. Y. Zhang, X. G. Yang, and C. Y. Wang, "Liquid water removal from a polymer electrolyte fuel cell," *J. Electrochem. Soc.*, vol. 153, no. 2, pp. A225–A232, 2006.

[27] G. Dotelli, R. Ferrero, P. G. Stampino, and S. Latorrata, "Analysis and compensation of PEM fuel cell instabilities in low-frequency EIS measurements," *IEEE Trans. Instrum. Meas.*, vol. 63, no. 7, pp. 1693–1700, Jul. 2014.